Turbulence-Model Predictions for Turbulent Boundary Layers

P. G. SAFFMAN* AND D. C. WILCOX†
Applied Theory, Inc., Los Angeles, Calif.

A set of turbulence model equations, originally postulated by Saffman, forms the basis of this three-part study of steady turbulent-boundary-layer structure above a flat plate. In one part of the study the turbulence equations are integrated through the viscous sublayer by means of time-marching numerical integration techniques and the constant in the law of the wall is predicted as a function of wall roughness. In a second part, the Van Driest compressible law of the wall is deduced by classical mathematical methods. Then, using the Van Driest law as a wall boundary condition, the model equations are integrated through the entire boundary layer, again by time-marching methods, for a freestream Mach number of 2.96.

1. Introduction

INCREASINGLY, turbulent-flow studies have concentrated on phenomenological-model equations describing turbulent motion. The most promising approach seeks rate equations which describe evolution of the Reynolds stresses; development of equations of this type has progressed for both low- and high-speed flows.[1-5] This paper focuses upon one such set of turbulence-model equations originally devised by Saffman[2] and subsequently modified by Wilcox and Alber[3] to account for the effects of compressibility; the model equations are based on the hypothesis that transfer of momentum and heat by turbulence can be described by an eddy viscosity which is a function of two turbulence densities, viz, an energy density, e, and a pseudovorticity density, Ω. Previous work [2,3] has concentrated mostly on formulation of the nonlinear diffusion equations satisfied by the turbulence densities; included in the present study is some model development which is directed primarily to the boundary conditions imposed at or near a solid boundary. As a result, uncertainties regarding boundary conditions have been eliminated. A concurrent study has been made of the predictions of the model equations for boundary layers on a flat plate under both compressible and incompressible flow conditions.

Past studies have left at least two areas of boundary-condition uncertainty. On the one hand, Saffman[2] indicated that the most natural boundary conditions for the mean velocity and the turbulence densities follow from matching to the law of the wall. Matching is valid for the incompressible Saffman model because law-of-the-wall behavior near a solid boundary is contained within the equations; however, Wilcox and Alber[3] did not generalize the matching concept for compressible flows. On the other hand, for some applications, integration through the sublayer might be necessary (because of, e.g., numerical reasons or sublayer-structure uncertainties). Thus, the question of boundary conditions for the turbulence densities appropriate to a solid boundary was considered briefly by Saffman and in a little more detail by Wilcox and Alber. Although the boundary condition on e is straightforward (it vanishes at solid boundaries), both studies fall short of specifying a boundary condition on the vorticity density.

The present work has eliminated these two areas of uncertainty, thereby facilitating detailed study of flat-plate-boundary-layer structure. The turbulence-model equations are presented in Sec. 2, and in Sec. 3 a boundary condition for Ω at a solid surface is determined; predicted incompressible sublayer structure also is studied and compared with experimental observations. The Van Driest compressible law of the wall[6] is deduced from the model equations in Sec. 4 whereby matching to the law of the wall is extended to compressible flows. Included in Sec. 5 are the results of a Mach 3 flat-plate-boundary-layer calculation in which the Van Driest law is employed as a boundary condition at the plate surface.

2. The Model Equations

The mean conservation equations of mass, momentum, and energy used in the present study are

$$\partial\bar{\rho}/\partial t+(\partial/\partial x_j)(\bar{\rho}\tilde{u}_j)=0 \tag{1}$$

$$(\partial/\partial t)(\bar{\rho}\tilde{u}_i)+(\partial/\partial x_j)(\bar{\rho}\tilde{u}_j\tilde{u}_i)=-\partial\bar{P}/\partial x_i+(\partial/\partial x_j)(T_{ij}-\langle\rho u_i u_j\rangle) \tag{2}$$

$$(\partial/\partial t)(\bar{\rho}\tilde{E})+(\partial/\partial x_j)(\bar{\rho}\tilde{u}_j\tilde{E})=(-\bar{P}\delta_{ij}+T_{ij}-\langle\rho u_i u_j\rangle)\partial\tilde{u}_i/\partial x_j+\gamma(\partial/\partial x_j)[\bar{\mu}(\partial\tilde{E}/\partial x_j)/Pr_L-\langle\rho u_j\tilde{E}'\rangle] \tag{3}$$

where $\tilde{u}_i$ and $\tilde{E}$ are the mass averaged velocity and internal energy, respectively, defined as

$$\tilde{u}_i=w_i-u_i=\langle\rho w_i\rangle/\bar{\rho} \tag{4}$$

$$\tilde{E}=E-\tilde{E}'=\langle\rho E\rangle/\bar{\rho} \tag{5}$$

The quantities w_i and E are instantaneous velocity and internal energy while u_i and $\tilde{E}'$ denote the difference between instantaneous and mass averaged values as indicated in Eqs. (4) and (5). Also, $\bar{P}$, T_{ij}, $\bar{\mu}$, γ and Pr_L denote mean pressure, mean laminar stress tensor, mean molecular viscosity, specific heat ratio and laminar Prandtl number, respectively.

The Reynolds stress tensor, τ_{ij}, is expressed in terms of an eddy viscosity, ε, as

$$\tau_{ij}\equiv-\langle\rho u_i u_j\rangle=\bar{\rho}\varepsilon[\partial\tilde{u}_i/\partial x_j+\partial\tilde{u}_j/\partial x_i-2/3\partial\tilde{u}_k/\partial x_k\delta_{ij}]-2/3\bar{\rho}e\,\delta_{ij} \tag{6}$$

where e is the specific turbulent energy defined as

$$e\equiv\tfrac{1}{2}\langle\rho u_i u_i\rangle/\bar{\rho} \tag{7}$$

Similarly, the turbulent heat flux vector becomes

$$-\langle\rho u_j\tilde{E}'\rangle=\bar{\rho}\varepsilon(\partial\tilde{E}/\partial x_j)/Pr_T \tag{8}$$

where Pr_T is the turbulent Prandtl number.

The eddy viscosity is assumed to be a function of local properties of the turbulence, namely e, and a pseudovorticity, Ω, which are assumed to satisfy the following nonlinear diffusion equations

$$(\partial/\partial t)(\bar{\rho}e)+(\partial/\partial x_j)(\bar{\rho}\tilde{u}_j e)=[\alpha^*(2S_{ij}S_{ij})^{1/2}-\beta^*\rho\Omega]\rho e+(\partial/\partial x_j)[(\bar{\mu}+\sigma^*\bar{\rho}\varepsilon)\partial e/\partial x_j]-\xi\bar{\rho}e\,\partial\tilde{u}_k/\partial x_k \tag{9}$$

Received May 5, 1973; revision received October 11, 1973. J. G. Trulio of Applied Theory, Inc. contributed invaluable guidance in the numerical work done in this study. Research was sponsored by the Air Force Aerospace Research Laboratories, Air Force Systems Command, U.S. Air Force, Contract F33615-72-C-1780.

Index category: Boundary Layers and Convective Heat Transfer—Turbulent.

* Consultant; also Professor of Applied Mathematics, California Institute of Technology.

† Staff Scientist; present affiliation: owner, DCW Industries, Sherman Oaks, Calif. Member AIAA.

$$(\partial/\partial t)(\bar{\rho}\Omega^2)+(\partial/\partial x_j)(\bar{\rho}\tilde{u}_j\Omega^2)=[\alpha\{(\partial\tilde{u}_i/\partial x_j)(\partial\tilde{u}_i/\partial x_j)\}^{1/2}-\beta\rho\Omega]\rho\Omega^2+(\partial/\partial x_j)[(\bar{\mu}+\sigma\bar{\rho}\varepsilon)\,\partial\Omega^2/\partial x_j] \quad (10)$$

where S_{ij} is the mean rate of strain tensor.

Equations (9) and (10) incorporate the essential physical idea that turbulence is convected by the mean flow, amplified by interaction with the mean rate of strain, destroyed by its self-interaction, and diffused by its own velocities. The numbers α, α^*, β, β^*, σ, σ^*, ξ and Pr_T are assumed to be universal constants. The equations are then closed by the relation

$$\varepsilon = e/\bar{\rho}\Omega \quad (11)$$

With the exception of ξ and Pr_T, the values of the universal constants can be fixed by very general arguments[2,3] and the given values used in all calculations in this study are given by

$$\left.\begin{aligned}&\sigma=\sigma^*=\tfrac{1}{2}\\&\alpha^*=0.3\\&\beta^*=\alpha^{*2}\\&\tfrac{5}{3}\leqq\beta/\beta^*\leqq 2\\&\alpha=\alpha^*[\beta/\beta^*-4\sigma\kappa^2/\alpha^*]\end{aligned}\right\} \quad (12)$$

where κ is the Kármán constant. To determine the value of ξ, a variety of supersonic and hypersonic flows has been considered.[3] Comparison with experimental data covering a Mach number range from 1.7 to 8.0 indicates a value of 2.5. Based on an argument presented at the end of Sec. 4 the turbulent Prandtl number, Pr_T, has been chosen as 0.89. Thus, the compressible model equations constitute a closed set of phenomenological equations in which the freedom to adjust the constant parameters is severely limited.

To facilitate integration through the viscous sublayer and to eliminate possible numerical difficulties at a turbulent- nonturbulent interface which might be encountered in performing a finite-difference solution, molecular diffusion terms appear in Eqs. (2, 3, 9, and 10). Adding viscous terms in the manner indicated is a simple and, at least to date, satisfactory approach which does not involve the addition of further arbitrary constants.

3. Viscous Sublayer Structure

For incompressible sublayer flow, the equations of motion Eqs. (1–11) simplify to the following ordinary differential equations [hereafter, as convenient, mass average (tilda) and conventional time average (overhead bar) symbols will be dropped]

$$(\nu+e/\omega)\,du/dy=\tau_w/\rho \quad (13)$$

$$(\alpha^*|du/dy|-\beta^*\omega)e+(d/dy)[(\nu+\sigma^*e/\omega)\,de/dy]=0 \quad (14)$$

$$(\alpha|du/dy|-\beta\omega)\omega^2+(d/dy)[(\nu+\sigma\varepsilon/\omega)\,d\omega^2/dy]=0 \quad (15)$$

where τ_w is the surface stress, ν is kinematic viscosity, y is distance normal to the solid boundary, and ω is defined by $\omega=\rho\Omega$. Three boundary conditions to which solutions of Eqs. (13–15) must be subjected are obtained by matching to the law of the wall so that

$$\left.\begin{aligned}&u\to u_\tau[\kappa^{-1}\log(u_\tau y/\nu)+C]\\&e\to\tau_w/\rho\alpha^*\\&\omega\to u_\tau/\kappa\alpha^* y\end{aligned}\right\}\ \text{as}\ u_\tau y/\nu\to\infty \quad (16)$$

where C is a constant whose value depends upon the nature of the wall and u_τ denotes the friction velocity, $u_\tau=(\tau_w/\rho)^{1/2}$. An additional boundary condition can be specified at the bounding surface, $y=0$, where the turbulent energy must vanish. Since equation set (13–15) is of fifth order, one more boundary condition is required for a well-posed two-point-boundary-value problem. Saffman[2] has proposed such a boundary condition, i.e.,

$$\omega=(\tau_w/\alpha^*\mu)S(z_o u_\tau/\nu) \qquad \text{at solid boundaries} \quad (17)$$

where $S(z_o u_\tau/\nu)$ is a universal function of the roughness height of the wall, z_o (Saffman postulated existence of the function S but did not determine its behavior or even its value for a smooth wall).

The value of C which appears in the law of the wall, Eq. (16), also depends on z_o, indicating a correspondence between the value of the constant C and the function $S(z_o u_\tau/\nu)$; hence, to establish the dependence of S upon the roughness height the following sequence has been observed: 1) Assume a value for S and solve the resulting two-point-boundary-value problem. 2) Using the solution to the boundary-value problem, determine the constant C. 3) Knowing C, appeal to experimental data (Schlichting[7]) to find the nondimensional roughness height, $z_o u_\tau/\nu$.

The boundary-value problem was then solved with the aid of a time-marching finite-difference code (AFTON 1PSL) for one-dimensional motion. Unsteady terms $\partial e/\partial t$ and $\partial\Omega^2/\partial t$ were added to the turbulent energy and vorticity equations, respectively, and the solution to the boundary value problem was generated as the steady limit of a time-varying field, i.e., as the unsteady terms approached zero. Numerical solutions were also generated by solving the two point boundary value problem by shooting from infinity towards the wall; no significant difference in the results was detected.

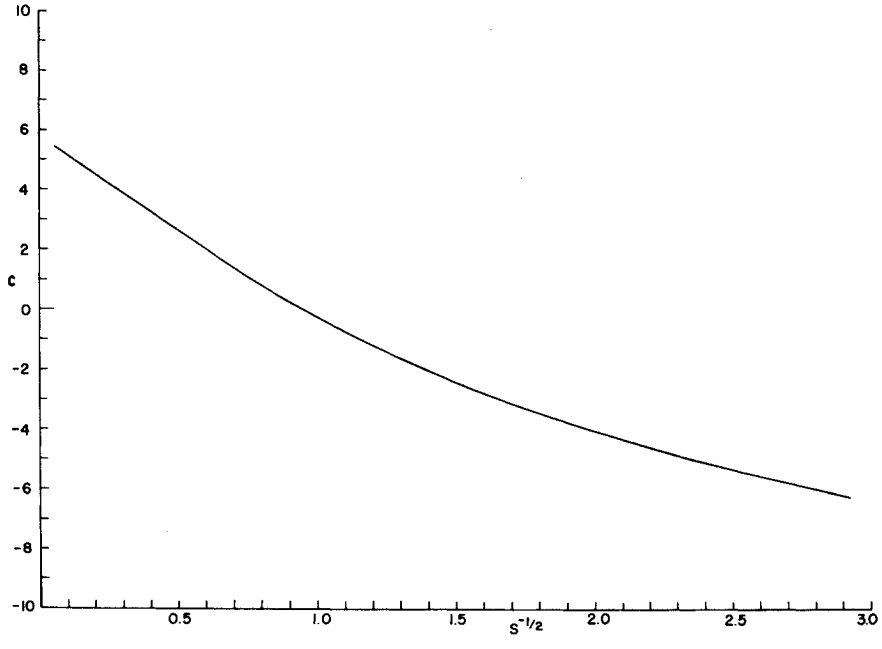

Fig. 1 The value of C as a function of $S^{-1/2}$ as determined from numerical solution of the sublayer equations.

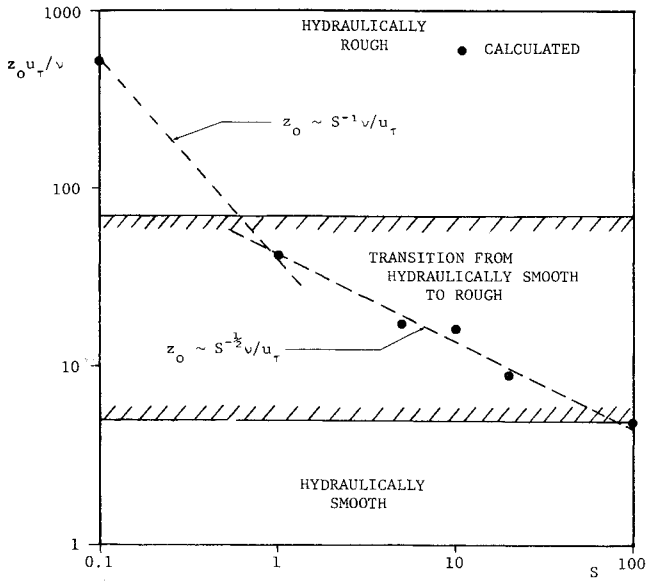

Fig. 2 Correlation of roughness height and the value of the vorticity density at a solid boundary; calculated values inferred from the numerical results relating S and C and experimental data relating z_o and C.

The value of S was varied from $\frac{1}{10}$ to 400, and the resulting dependence of C upon $S^{-1/2}$ is shown in Fig. 1. (The choice of $S^{-1/2}$ for the abscissa was suggested by theoretical considerations given below. Numerical considerations precluded calculation for values of $S^{-1/2}$ less than 0.05, but an extrapolation to $S^{-1/2}=0$ appears warranted.) The dependence of $z_o u_\tau/\nu$ on S inferred from the experimental data is shown in Fig. 2. The roughness height is a monotonically decreasing function of S, and a value of $S = 100$ is sufficient to reach the hydraulically smooth regime. The corresponding value of C of 5.05 is within the generally accepted range for smooth walls of between 5.0 and 5.5. The obvious implication of the analysis is that

$$S(z_o u_\tau/\nu) \to \infty \quad \text{as} \quad z_o u_\tau/\nu \to 0 \tag{18}$$

and extrapolation of the numerical data of Fig. 1 indicates that for infinite S the constant C will tend to a value of about 5.7. As S is a measure of the fluctuation frequency at the wall, intuition suggests that $S = \infty$ is the proper limit for a *perfectly* smooth wall.

Calculated velocity profiles for several values of S are shown in Fig. 3, which also includes experimental data for a smooth wall.[8] For $S = 100$, the computed velocity profile closely agrees with

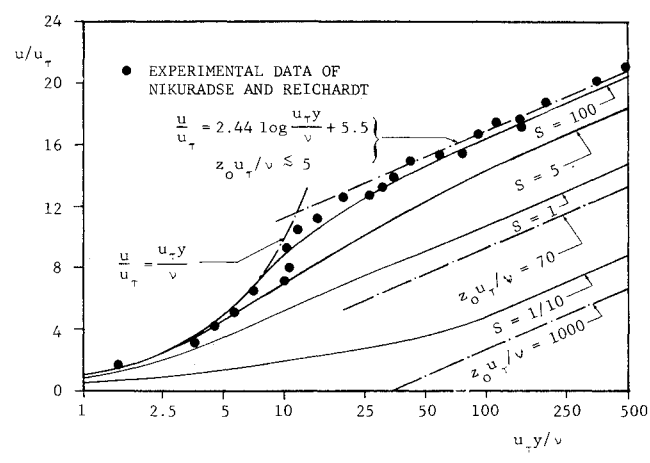

Fig. 3 Comparison of calculated sublayer velocity profiles with experimental data.

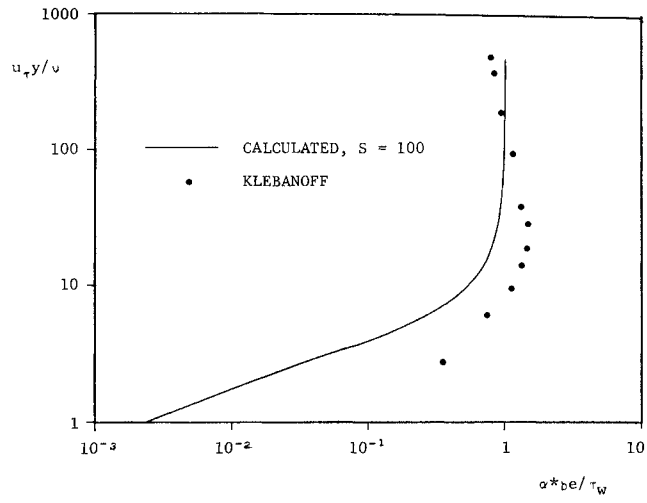

Fig. 4 Comparison of calculated turbulent energy in the viscous sublayer with experimental data.

the experimental data. The various profiles show that the value of the pseudovorticity density at a solid boundary affects predicted structure of the turbulent boundary layer well beyond the sublayer. Figure 4 compares specific turbulent energy with experimental data[9]; the computed and measured data agree reasonably well, particularly at the outer sublayer edge.

The variation of e near $y = 0$ appears to differ drastically from the prediction of Wilcox and Alber that e is linear with y as $y \to 0$. However, the discrepancy vanishes upon examination of the limiting form of the sublayer structure as $y \to 0$. For large S, there is a thin inner layer near $y = 0$ whose thickness is of order $S^{-1/2}\nu/u_\tau$. Inspection of Fig. 2 shows that, on approaching the hydraulically smooth regime, the roughness height is also of order $S^{-1/2}\nu/u_\tau$, indicating that the inner layer is a region where detailed wall-roughness effects dominate; this layer will hence be referred to as the "roughness layer." The appearance of the roughness layer is physically realistic since wall roughness consists of small protrusions from the surface; one would thus expect the size and shape of the protrusions to influence local flow conditions to distances of the order of a characteristic protrusion dimension. In the roughness layer the production and turbulent diffusion terms in Eqs. (14) and (15) can be neglected; the turbulence densities behave according to

$$\omega = (\tau_w S/\alpha^* \mu)\eta^{-2} \tag{19}$$

$$e \sim [\eta^n - \eta^m] \tag{20}$$

where

$$\eta \equiv 1 + \frac{1}{2}\left(\frac{\alpha^*}{5}\frac{\beta}{\beta^*}S\right)^{1/2}\frac{u_\tau y}{\nu} \tag{21}$$

and the exponents n and m are given by

$$\left.\begin{aligned} n &= \tfrac{1}{2}[1+(1+80\beta^*/\beta)^{1/2}] \\ m &= \tfrac{1}{2}[1-(1+80\beta^*/\beta)^{1/2}] \end{aligned}\right\} \tag{22}$$

Equation (20) shows that within the roughness layer the turbulent energy passes from linear variation with y when $S^{1/2}u_\tau y/\nu \to 0$ to the more rapid increase given by y^n when $S^{1/2}u_\tau y/\nu \to \infty$. Since the roughness-layer thickness becomes vanishingly small as S becomes large, the latter behavior will characterize the variation of e in the sublayer near smooth solid boundaries as exemplified in Fig. 4. The exponent n varies between 3.70 and 4.00 for the permissible range of values of β/β^* given in Eq. (12); hence, contrary to the claim of Wilcox and Alber,[3] the Saffman equations possess physically acceptable solutions for e in the viscous sublayer. The results obtained here also indicate claims of Baum[10] that the Saffman model does not work well for incompressible boundary layers are wrong. The erroneous conclusion drawn in Baum's study appears to be caused by the use

of incorrect boundary conditions and an unsuitable choice of viscous modifications for the sublayer.

4. The Compressible Law of the Wall

We turn now to the behavior of the compressible form of the model equations in the so-called wall layer, namely, the region sufficiently close to the solid boundary for neglect of convective terms and far enough distant from the boundary for molecular diffusion terms to be dropped. The equations of motion for compressible flow in the wall layer are

$$(e/\Omega)\,du/dy = \tau_w \tag{23}$$

$$(d/dy)[(e/\Omega)(d/dy)(h/Pr_T+\tfrac{1}{2}u^2)] = 0 \tag{24}$$

$$\left(\alpha^*\left|\frac{du}{dy}\right|-\alpha^{*2}\rho\Omega\right)\rho e+\sigma^*\frac{d}{dy}\left[\frac{e}{\Omega}\frac{de}{dy}\right]=0 \tag{25}$$

$$\left(\alpha\left|\frac{du}{dy}\right|-\beta\rho\Omega\right)\rho\Omega^2+\sigma\frac{d}{dy}\left[\frac{e}{\Omega}\frac{d\Omega^2}{dy}\right]=0 \tag{26}$$

Equations (23–26) can be made much more tractable by regarding u as the independent variable rather than y. Hence, the equations for the turbulence densities reduce to

$$\sigma^* d^2e/du^2+[1-\alpha^*\rho e/\tau_w]\alpha^*\rho e/\tau_w = 0 \tag{27}$$

$$\sigma d^2\Omega^2/du^2+[\alpha-(\beta/\alpha^*)\alpha^*\rho e/\tau_w]\rho\Omega^2/\tau_w = 0 \tag{28}$$

The energy equation can be trivially integrated and for a perfect gas integration yields the relation

$$\rho_w/\rho = 1+B(u/U_\infty)-A^2(u/U_\infty)^2 \tag{29}$$

where ρ_w is the fluid density corresponding to the temperature of the bounding surface, T_w, and U_∞ is the velocity at the edge of the boundary layer; the constants A and B are given by the expressions

$$A^2 = \tfrac{1}{2}(\gamma-1)Pr_T M_\infty{}^2 T_\infty/T_w \tag{30}$$

$$B = -Pr_T q_w U_\infty/C_p T_w \tau_w \tag{31}$$

where q_w is the heat flux from the fluid to the wall. The quantities T_∞ and M_∞ are the freestream temperature and Mach number, respectively, while γ is the specific heat ratio and C_p the specific heat. Assuming a solution of the form

$$e = \Gamma\tau_w/\rho \tag{32}$$

where Γ is an unknown constant, we find by combining Eqs. (27) and (32) that

$$\Gamma = [1-\tfrac{1}{2}(\gamma-1)Pr_T(\sigma^*/\alpha^*)M_\infty{}^2 c_f]/\alpha^* \tag{33}$$

The term $M_\infty{}^2 c_f$ is very small for flows of practical interest and therefore

$$\Gamma \approx 1/\alpha^* \tag{34}$$

The turbulent energy can now be eliminated from Eq. (28) for Ω by combining Eqs. (28, 29, 32, and 34). The resulting equation is

$$d^2\Omega^2/du^2-4(\kappa/u_\tau)^2[1+B(u/U_\infty)-A^2(u/U_\infty)^2]^{-1}\Omega^2 = 0 \tag{35}$$

Finally, let $v \equiv u/U_\infty$ and $R \equiv 2\kappa U_\infty/u_\tau$. Equation (35) can then be written in the simplified form

$$d^2\Omega^2/dv^2-R^2[1+Bv-A^2v^2]^{-1}\Omega^2 = 0 \tag{36}$$

Equation (36) is a spheroidal wave equation whose solutions could be expressed in terms of Legendre functions of complex order; more useful results are obtained by the WKBJ method, which yields the following approximate solution for large R

$$\Omega^2 \sim D^2(1+Bv-A^2v^2)^{1/4}\exp\left[\pm\frac{R}{A}\sin^{-1}\left(\frac{2A^2v-B}{(B^2+4A^2)^{1/2}}\right)\right] \tag{37}$$

where D is a constant of integration. Recalling Eq. (23), combining it with Eqs. (32, 34, and 37) and integrating over y we arrive at the result that

$$\int(1+Bv-A^2v^2)^{7/8}\exp\left[\frac{R}{2A}\sin^{-1}\left(\frac{2A^2v-B}{(B^2+4A^2)^{1/2}}\right)\right]dv = \alpha^*\rho_w Dy/U_\infty \tag{38}$$

The ambiguity in sign which first appeared in Eq. (37) has been removed by noting that, for the special case of a flat-plate boundary layer, d^2v/dy^2 will be negative for all values of y. For very large R the integral in Eq. (38) can be replaced by its asymptotic expansion and therefore

$$\frac{4A^2}{R}[1+Bv-A^2v^2]^{11/8}\exp\left[\frac{R}{2A}\sin^{-1}\left(\frac{2A^2v-B}{(B^2+4A^2)^{1/2}}\right)\right] \sim \alpha^*\rho_w Dy/U_\infty+\text{const} \tag{39}$$

Finally, we expand v in a perturbation series for large R as

$$v = R^{-1}v_0+\mu(R)v_1+\cdots; \qquad \mu(R) \ll R^{-1} \tag{40}$$

Combining Eqs. (39) and (40) the resulting solution for v_0 is given by

$$\frac{U_\infty}{A}\sin^{-1}\left(\frac{2A^2v_0-B}{(B^2+4A^2)^{1/2}}\right) = \frac{u_\tau}{\kappa}\log\frac{\kappa\alpha^*\rho_w Dy}{2A^2u_\tau}+\text{const} \tag{41}$$

Equation (41) is identical to the compressible law of the wall deduced by Van Driest[6] provided

$$D = 2A^2\tau_w/\kappa\alpha^*\rho_w\mu_w \tag{42}$$

where μ_w is the fluid molecular viscosity at temperature T_w. Therefore, in the limit of large Reynolds number, i.e.,

$$R \equiv 2\kappa U_\infty/u_\tau \to \infty \tag{43}$$

the velocity in a boundary layer very close to the boundary is predicted by our model equations to behave as

$$\frac{U_\infty}{A}\sin^{-1}\left[\frac{2A^2(u/U_\infty)-B}{(B^2+4A^2)^{1/2}}\right] = \frac{u_\tau}{\kappa}\log\frac{u_\tau y}{\nu_w}+\text{const} \tag{44}$$

Also, combining Eqs. (32) and (34) the turbulent energy will vary according to the expression

$$\rho e = \tau_w/\alpha^* \tag{45}$$

Inserting Eq. (44) into Eq. (23) and combining the result with Eq. (45) leads to

$$\rho\Omega = (\rho_w/\rho)^{1/2}u_\tau/\alpha^*\kappa y \tag{46}$$

Equations (44–46) can be used as boundary conditions in the sense of matched asymptotic expansions, thus circumventing the process of integration of the turbulence equations down through the viscous sublayer.

As a final note, the results obtained in this section make it possible to fix the value of the turbulent Prandtl number, Pr_T. That is, good correlation of experimental data with Eq. (44) is obtained when the value of A is calculated from

$$A^2 = \tfrac{1}{2}(\gamma-1)rM_\infty{}^2 T_\infty/T_w \tag{47}$$

where r is the recovery factor.[11,12] Comparison of Eqs. (30) and (47) implies that Pr_T should be equal to 0.89, the accepted value of r.

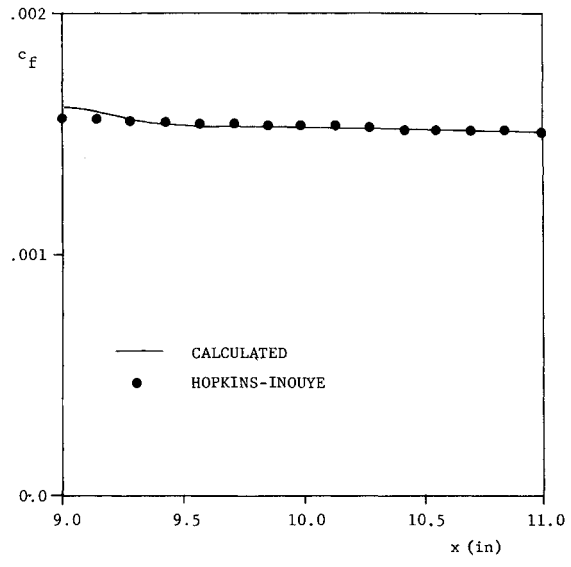

Fig. 5 Skin friction as a function of distance from the leading edge of a flat plate; freestream Mach number $M_\infty = 2.96$; freestream Reynolds number per unit length, 1.49×10^6 in.$^{-1}$.

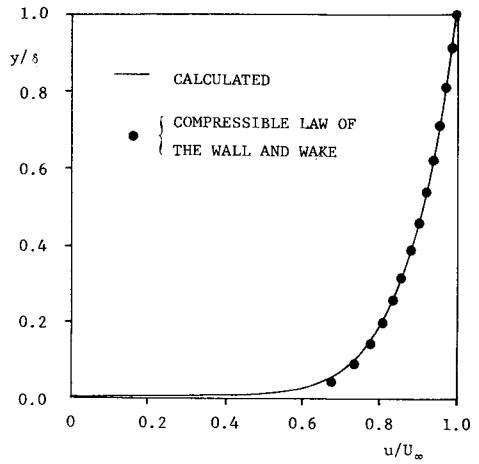

Fig. 6 Velocity profile for a supersonic turbulent flat plate boundary layer; freestream Mach number, $M_\infty = 2.96$; Reynolds number based on momentum thickness, $Re_\theta = 15{,}300$.

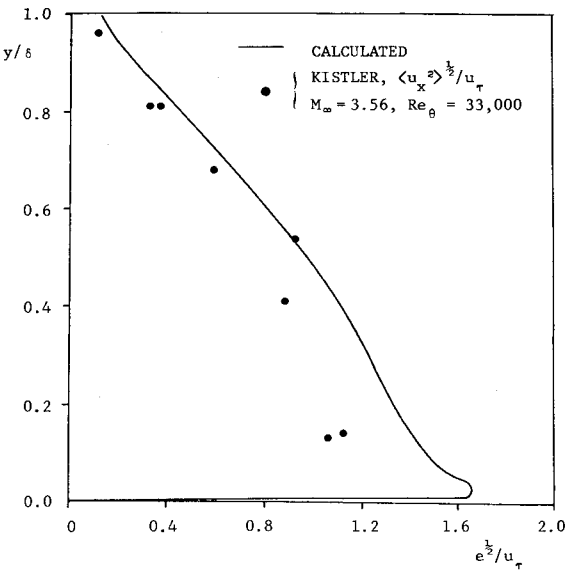

Fig. 8 Variation of turbulence intensity through a supersonic turbulent flat plate boundary layer; freestream Mach number, $M_\infty = 2.96$; Reynolds number based on momentum thickness, $Re_\theta = 15{,}300$.

5. Numerical Computation of Supersonic Turbulent Flow Over an Adiabatic Flat Plate

The turbulence-model equations presented in Sec. 2 have been incorporated into a time-marching finite-difference code (AFTON 2P) for two-dimensional-plane fluid motion.[13-15] The modified code (AFTON 2PT) has been used to calculate Mach 2.96 turbulent-boundary-layer flow above an adiabatic flat plate using the law-of-the-wall boundary conditions derived in Sec. 4. Details of the numerical process have been given elsewhere.[15]

The inherent economy of matching to the law of the wall for numerical work is exemplified by the fact that only 14 finite-difference mesh points were used to define the boundary layer, whereas 30 to 40 points would otherwise have been required. The reduction in mesh point density is made possible because the first mesh line (along which the law-of-the-wall boundary condition developed in Sec. 4 is applied) need be no closer than about 5% of a boundary-layer thickness, δ, above the plate (0.05δ was used for the computation reported here).

The calculated skin-friction coefficient, c_f, is shown in Fig. 5. Effects of a slight error in c_f introduced at the upstream boundary of the finite-difference mesh are observed to persist to about two-boundary-layer thicknesses ($\delta \approx \frac{1}{6}$ in.) downstream of the boundary. Beyond that point, calculated values of c_f are within 2% of measured values. Computed boundary-layer thickness and momentum thickness also fall within 2% of corresponding experimentally measured values.

The AFTON-calculated velocity, temperature, turbulent energy, and shear stress profiles are shown in Figs. 6–10 at a position where the Reynolds number based on momentum thickness is 15,300. In Fig. 6, the calculated velocity profile differs from the compressible law of the wall and wake[11,12] profile by less than 2% at all points. The computed velocity profile exhibits experimentally observed behavior in both the law-of-the-wake and law-of-the-wall regions as can be seen from Fig. 7 where sublayer coordinates, u/u_τ and $u_\tau y/\nu_w$ are used.

The calculated profile of specific turbulent energy, e, compares less directly with measured data than does the velocity profile since rms velocity fluctuation data are available only for the streamwise velocity component (and even then at slightly higher Mach and Reynolds numbers than those of the computed field).[16] The calculated e-profile and measured values of $\langle u_x^2 \rangle$ are compared in Fig. 8. Except very close to the plate, where the data are of questionable accuracy, the average difference between computed and measured values is approximately 10%.

In Fig. 9 the computed temperature profile is shown to resemble the Crocco temperature profile which is identical to Eq. (29) when $Pr_T = r$. As would be expected from the comments at the end of Sec. 4, the computed recovery factor is 0.89, identical to the accepted value for turbulent flow. As inspection of Fig. 10 shows, the calculated-shear-stress profile is within

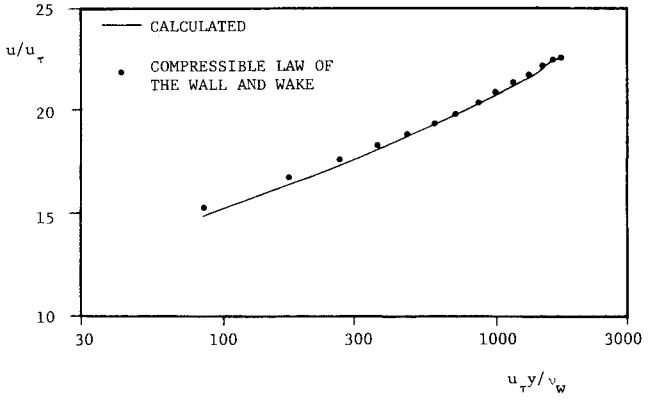

Fig. 7 Velocity profile for a supersonic turbulent flat plate boundary layer in sublayer coordinates; freestream Mach number, $M_\infty = 2.96$; Reynolds number based on momentum thickness, $Re_\theta = 15{,}300$.

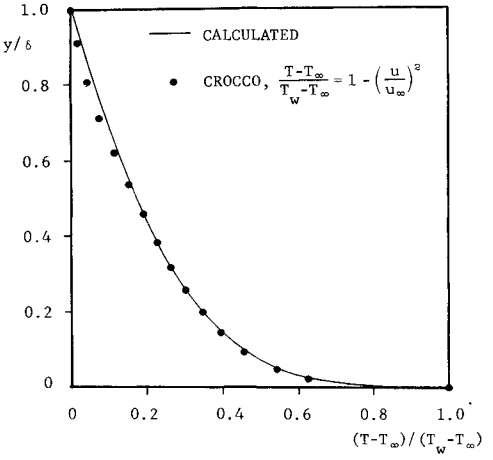

Fig. 9 Temperature profile for a supersonic turbulent flat plate boundary layer; freestream Mach number, $M_\infty = 2.96$; Reynolds number based on momentum thickness, $Re_\theta = 15{,}300$.

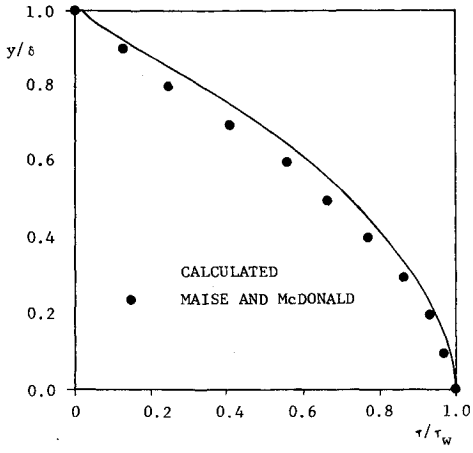

Fig. 10 Shear stress profile for a supersonic turbulent flat plate boundary layer; freestream Mach number $M_\infty = 2.96$; Reynolds number based on momentum thickness, $Re_\theta = 15{,}300$.

8% of the Maise and McDonald[11] correlation of experimental data.

We emphasize that this remarkable agreement between experiment and theory was accomplished with only one adjustable parameter at our disposal, namely, the turbulent Prandtl number.

6. Summary and Conclusions

The results presented in Sec. 3–5 show that the Saffman turbulence-model equations accurately predict many features of turbulent boundary layers. Principal results of the study are summarized below.

Study of the incompressible sublayer has revealed a simple and natural way of including wall roughness effects in the model; the equations predict the existence of a region below the sublayer in which wall roughness effects would dominate.

The Van Driest compressible law of the wall has been deduced from the model equations which provides a consistency check of the model with physical reality and constitutes the basis for extending, to compressible flows, the concept of matching to the law of the wall.

Calculated Mach 2.96 flat-plate-boundary-layer structure, using the compressible-law-of-the-wall boundary condition, agrees closely with experimental observations. Computed skin-friction, boundary-layer thickness and momentum thickness are within 2% of corresponding experimental data while turbulent-energy and shear-stress profiles generally differ from measured profiles by no more than 10%. The calculated velocity profile virtually duplicates experimentally observed behavior in both the law-of-the-wall and the law-of-the-wake regions.

In addition to the conclusion that the Saffman turbulence model accurately predicts flat-plate boundary-layer properties, a second inference can be made. Specifically, the close correspondence between the Saffman-model equations and other two-parameter modelling schemes noted by Wilcox and Alber[3] indicates that the results of the present study have general applicability for two-parameter turbulence models.

References

[1] Kolmogorov, A. N., "Equations of Turbulent Motion of an Incompressible Fluid," *Izvestia Academy of Sciences, USSR; Physics,* Vol. 6, Nos. 1 and 2, 1942, pp. 56–58.

[2] Saffman, P. G., "A Model for Inhomogeneous Turbulent Flow," *Proceedings of the Royal Society, London,* Vol. A317, 1970, pp. 417–433.

[3] Wilcox, D. C. and Alber, I. E., "A Turbulence Model for High Speed Flows," *Proceedings of the 1972 Heat Transfer and Fluid Mechanics Institute,* 1972, pp. 231–252.

[4] Rotta, J. C., "Statistiche Theorie Nichthomogener Turbulenz," *Zeitschrift für Physik,* Vol. 131, 1951, pp. 51–77.

[5] Donaldson, C. duP., "Calculation of Turbulent Shear Flows Through Closure of the Reynolds Equations by Invariant Modeling," ARAP Rept. 127, 1968, Aeronautical Research Associates of Princeton, Princeton, N.J.

[6] Van Driest, E. R., "Turbulent Boundary Layer in Compressible Fluids," *Journal of Aeronautical Science,* Vol. 18, 1951, pp. 145–160, 216.

[7] Schlichting, H., *Boundary Layer Theory,* 4th ed., McGraw-Hill, New York, 1960, p. 523.

[8] Schlichting, H., *Boundary Layer Theory,* 4th ed., McGraw-Hill, New York, 1960, p. 507.

[9] Klebanoff, P. S., "Characteristics of Turbulence in a Boundary Layer with Zero Pressure Gradient," Rept. 1247, 1955, NACA.

[10] Baum, E., "Semi-Annual Technical Report—Turbulent Wakes," TRW Rept. 32028-6001-RU-00, Dec. 1972, TRW Systems, Inc., Redondo Beach, Calif.

[11] Maise, G. and McDonald, H., "Mixing Length and Kinematic Eddy Viscosity in a Compressible Boundary Layer," AIAA Paper 67-199, New York, 1967.

[12] Hopkins, E. J. and Inouye, M., "An Evaluation of Theories for Prediction of Turbulent Skin Friction and Heat Transfer on Flat Plates at Supersonic and Hypersonic Mach Numbers," *AIAA Journal,* Vol. 9, No. 6, June 1971, pp. 993–1003.

[13] Trulio, J. G. and Walitt, L., "Numerical Calculations of Viscous Compressible Fluid Flow Around a Stationary Cylinder," CR-1465, 1970, NASA.

[14] Trulio, J. G., Walitt, L., and Niles, W. J., "Numerical Calculations of Viscous Compressible Fluid Flow Over a Flat Plate and Step Geometry," CR-1466, 1970, NASA.

[15] Wilcox, D. C., "Numerical Study of Separated Turbulent Flows," ATR-38-73-1, 1973, Applied Theory, Inc., Los Angeles, Calif.

[16] Kistler, A. L., "Fluctuation Measurements in a Supersonic Turbulent Boundary Layer," *The Physics of Fluids,* Vol. 2, No. 5, 1959, p. 290.